Available online at www.sciencedirect.com
SCIENCE DIRECT®
Journal of Catalysis 221 (2004) 204–212
JOURNAL OF CATALYSIS
www.elsevier.com/locate/jcat

Nitric oxide reduction by Cu nanoclusters supported on thin Al_2O_3 films

S. Haq, A. Carew, and R. Raval *

Surface Science Research Centre, The University of Liverpool, Liverpool L69 3BX, UK

Received 16 May 2003; revised 2 July 2003; accepted 2 July 2003

Abstract

The adsorption and reaction of NO on Cu clusters deposited on a 5 Å thick Al_2O_3 film, created by oxidation of a NiAl{110} crystal, have been studied using infrared, molecular beam, and scanning tunneling spectroscopies over the temperature range of 90–300 K. STM shows Cu clusters ranging in size from 20 to 40 Å and typically about 8 Å in height. Infrared spectra and molecular beam data show that the adsorption and reactivity of the particles are complex and very similar to those found on Cu single crystals. At 98 K, the infrared spectra are strongly coverage dependent and show the presence of monomeric NO adsorbed in two- and threefold sites, dimeric NO and N_2O species. Molecular beam data show that during adsorption N_2 and N_2O are produced into the gas phase, even at 98 K. A reaction mechanism is derived from these data, which indicate the formation of NO dimers as precursors to the dissociation products.

Keywords: Molecular beam; Infrared; STM; Cu clusters; Thin alumina film; Nitric oxide; Dinitrosyl species

1. Introduction

The use of extended single crystal surfaces to model and understand the basic elements of heterogeneous catalysis has been invaluable. This has resulted in a detailed understanding of how the reactivity of metal surfaces toward adsorbing species varies with key parameters, such as surface structure, temperature, pressure, and surface coverage. However, despite the success of these studies, recently there has been an increasing interest in replacing the single crystal with a model multicomponent system that realistically models the structure of a working catalyst. This involves creating small metal nanoparticles dispersed on an oxide support and subsequently exposing these to reactant species under clean and well-controlled conditions [1]. With these studies additional parameters such as particle size and influence of oxide support can be investigated. Additionally a comparison between single crystal and particle work is useful in understanding differences in reactivity between an extended surface and a particle surface. Interesting candidates for such comparative studies are simple σ-donor/π-acceptor diatomics such as CO and NO, where the bonding and coordination are extremely sensitive to surface structure and relatively easily measured using, for example, vibrational spectroscopy.

The interaction of NO with transition metal surfaces is of particular interest in catalysis, as it is a toxic pollutant produced in the exhaust emissions of automobiles. It is well established that NO is readily reduced using precious metal catalysts [2]. Surface science studies using extended single crystal surfaces have greatly aided in understanding its adsorption and decomposition on transition metals. The overall picture is that this interaction is rather complex, as the number and type of adsorbed species observed are regularly found to vary as a function of surface coverage and temperature [3]. The species observed to date include molecular NO adsorbed in atop, twofold, and threefold bridge positions. Additionally, bent NO and dinitrosyl species have also been observed as well as atomic species from its decomposition.

Although the precious metals Pt, Pd, and Rh are the most efficient in promoting the decomposition of NO, the base metals Cu and Ag show interesting reactivity. On these relatively unreactive metals the simple adsorption/desorption that is expected is not observed, and both have been clearly shown to facilitate N–O bond cleavage at temperatures as low as 85 K [4–14]. The interaction of NO with copper surfaces is particularly complex as a range of molecular species have been found to coexist at certain coverages. The earliest studies on polycrystalline and single crystal surfaces of Cu attributed the decomposition to arise from simple dissocia-

* Corresponding author.
E-mail address: r.raval@liv.ac.uk (R. Raval).

0021-9517/$ – see front matter
doi:10.1016/S0021-9517(03)00311-7

tive adsorption [4–8]. However, a detailed study by Brown et al. [10] using a combination of RAIRS, Molecular Beam, and TPD showed that the mechanism for NO dissociation on Cu{110} at low temperature included the formation of dimers which were the precursors to dissociation.

It is of interest to investigate if this mechanism is unique to extended surfaces or if it also operates for the interaction of NO with small Cu particles on an oxide support. A previous study using a combination of HREELS and TPD by Wu and Goodman [8] showed that Cu particles of ~ 65 Å diameter deposited on a thin alumina film were active for NO dissociation. The TPD results showed desorption of both N_2O and N_2 and it was suggested that these were produced from dissociated atomic N adatoms reacting with adsorbed NO and N, respectively. The vibrational spectra were complicated by the strong Al_2O_3 phonon losses. However, the similarity of the results with later work on single crystal surfaces tends to suggest a different reaction mechanism, although this needs to be proven. In this paper a detailed study is reported, based on the higher resolution of RAIRS compared to HREELS, combined with the absence of the inherent complexities associated with measuring vibrational modes of adsorbates on thin oxide films using HREELS due to strong phonon losses. Additionally, STM is used to directly image the Cu clusters to determine both the size and their spatial distribution and molecular beam experiments are used to study the dynamics of the adsorption and desorption.

2. Experimental

The experiments were conducted in two separate UHV chambers, one is a Omicron STM system and the other a combined RAIRS and Molecular Beam system. Both systems are equipped with the standard cleaning and characterisation techniques, including Ion gun, LEED, Auger, and Mass spectrometers. Infrared spectra were recorded using a Mattson FTIR spectrometer interfaced to the UHV chamber using KBr optics with an external MCT detector allowing access to a spectral range of 4000–700 cm^{-1}. All spectra were collected at 4 cm^{-1} resolution with the coaddition of 256 scans. The molecular beam apparatus has been described previously [10] and has been calibrated to give a flux of approximately 9×10^{12} molecules/s.

The stoichiometric NiAl{110} crystal ($8 \times 8 \times 2$ mm), oriented to better than 0.2° was purchased from Mateck, GmBH. For the infrared and molecular beam studies it was mounted using Ta support wires pushed into grooves in the side of the crystal, with a chromel/alumel thermocouple pair inserted into a small hole in one of the sides. For the STM studies it was mounted on a Ta transfer baseplate. The crystal was initially cleaned using numerous sputter (500 eV, 7 μA) and anneal cycles (1200 K) until it showed a sharp (1×1) LEED pattern and was free of contaminant as seen by AES. The 5 Å γ-alumina film was created by exposing the clean surface to oxygen and heating to 1200 K [15] and produced a sharp LEED pattern characteristic of the Al_2O_3 structure.

Copper was evaporated from a bead source made by melting high-purity Cu wire wrapped around a tungsten filament. The same source was used in the two chambers, and was operated at the same constant power and source to sample distance in each case to ensure that the sample received exactly the same flux in a given time. This was further confirmed by using identical mass spectrometers to measure the mass 63 and 65 Cu isotope signals in the two chambers. It should be noted that the evaporation fluxes and exposure times used in this work showed no change in the quality of the sharp oxide LEED pattern seen for the clean oxide surface, implying that thin films or high cluster coverages are not being formed, as also confirmed by the STM images.

3. Results

3.1. Scanning tunneling microscopy

It has previously been shown that the growth of Cu clusters on the 5 Å γ-alumina oxide film surface proceeds according to the Volmer–Weber mechanism; i.e., even for the lowest coverages 3-dimensional islands are formed [16,17]. The mean cluster size for this system changes according to a semilog scaling law with increasing Cu exposure [17]. The size and distribution of clusters, for the exposures used in these studies, are illustrated by the STM images shown in Fig. 1. The alumina film contains characteristic defect structures comprising reflectional and antiphase domain boundaries as well as step edges. For low Cu exposures the nucleation and growth of the clusters occur preferentially at these defect sites. The clusters are typically between 20 and 30 Å in size for a 0.22 L Cu dose. With increasing exposure the clusters increase in size and begin to coalesce into 3D islands of clusters. The height of these clusters is typically 6–8 Å, which equates to a few atomic layers of Cu. These dimensions are similar to those reported by Pang et al. for Cu deposited on α-Al_2O_3(0001) single crystal using AFM [18]. In our study we were unable to resolve the structure of individual particles; however, Worren et al. [16] have imaged the top facet of isolated crystalline clusters larger than 40 Å with atomic resolution and shown this to be (111) facet, although it should be noted that they were unable to image the morphology of smaller clusters.

3.2. Infrared spectroscopy

Adsorption of NO on the clean thin oxide film, prior to Cu deposition, was followed using both IR and molecular beam spectroscopies. The IR spectra showed no absorption bands and the molecular beam data showed no measurable uptake, suggesting that the oxide support is relatively inert to NO adsorption under the conditions of these experiments. The interaction of NO with the Cu clusters is followed as a

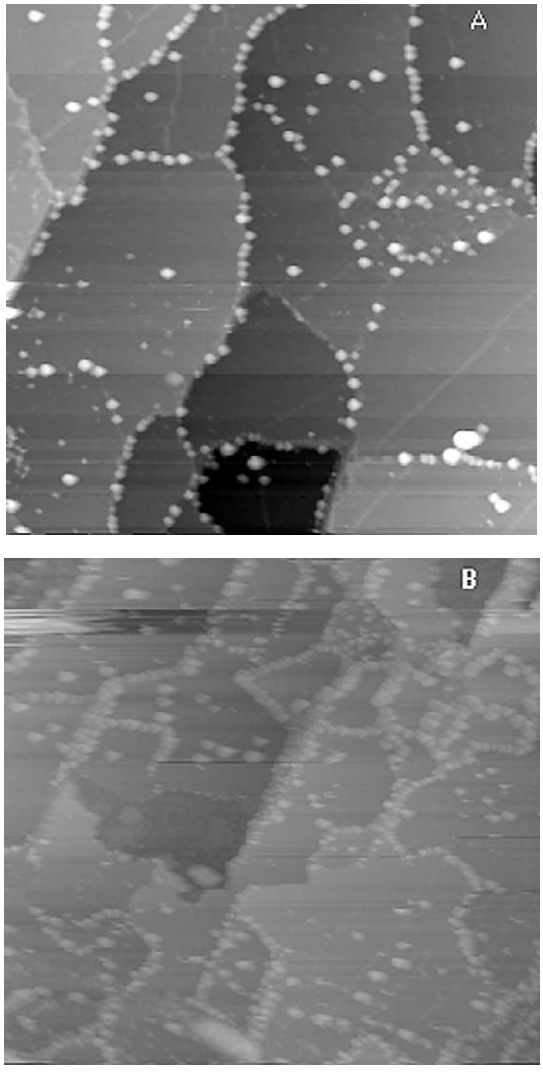

Fig. 1. STM images of Cu clusters formed on 5 Å alumina film, (A) after 0.22 L exposure of Cu, 1300 × 1300 Å^2, $I_t = 0.3$ nA, $V_t = 2$ V; (B) after 1.0 L exposure of Cu, 2000 × 2000 Å^2, $I_t = 0.2$ nA, $V_t = 2$ V.

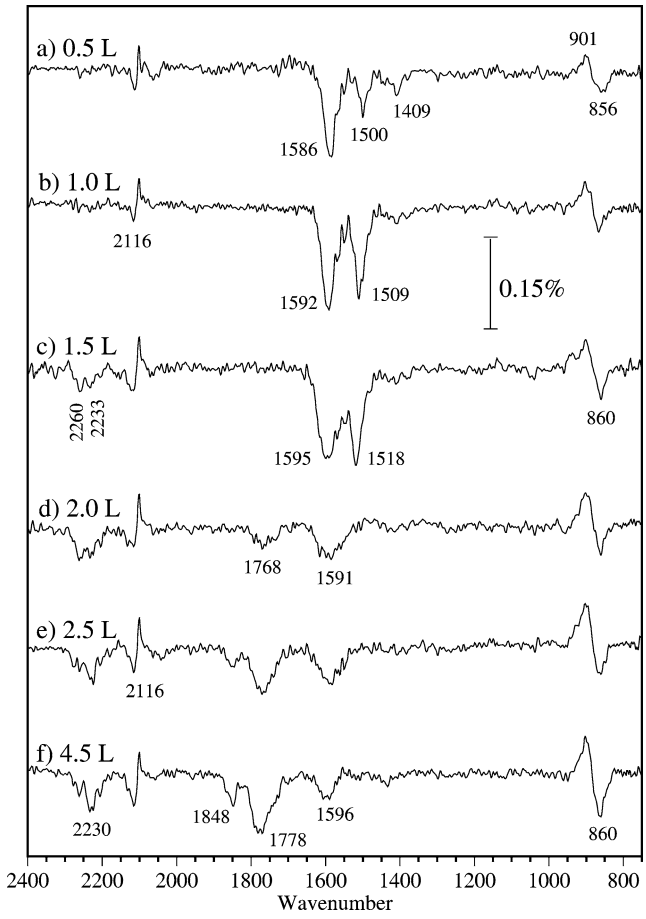

Fig. 2. RAIR spectra following adsorption of NO at 100 K on Cu particles produced from a 1.0 L Cu exposure.

function of increasing exposure using infrared spectroscopy. Fig. 2 shows the changes in the vibrational spectra as a function of increasing NO exposure at 100 K for Cu clusters formed from a 1.0 L Cu exposure.

First, it should be noted that the small derivative-like feature at 2116 cm^{-1} is due to small amounts of CO adsorbed from the background as the crystal is cooled to 100 K. A second point of note concerns the absorption band at 860 cm^{-1}; a δ(NO) for a bent NO species has been observed at a similar frequency on Cu{110} [10]. However, an Al_2O_3 dipole active optical phonon mode also occurs at this frequency [19]. The derivative-like nature of this band in most of the spectra suggests that it is probably associated with the phonon mode and shows that at least a part of the oxide film undergoes some change which lowers the frequency of this mode with exposure to NO. This effect has previously been reported and discussed by Frank et al. [19]. However, it is possible that for lower coverages of Cu (spectra a–c of Fig. 3) there may be a contribution from the δ(NO) of bent NO, as the lineshape does not correlate with a frequency shift of the phonon mode. The main bands observed in the spectral range of 1400–1900 cm^{-1} are all associated with internal υ(N–O) of adsorbed NO. The two bands observed at 2230 and 2260 cm^{-1} are in the frequency range expected for an N_2O species [10].

Initially three bands are observed at 1409, 1500, and 1586 cm^{-1} for a 0.5 L NO exposure indicating adsorption of NO into three chemically distinct environments. With increasing exposure up to 1.5 L the lowest frequency band attenuates as the band at 1500 cm^{-1} increases in intensity and shifts to 1518 cm^{-1}, while the intensity of the peak at 1586 cm^{-1} appears to remain constant but its frequency shifts to 1595 cm^{-1}. The shift of both bands is attributable to dipole–dipole coupling that is routinely seen for NO and CO adsorption. A distinct change in the spectra is seen with an exposure of over 1.5 L with the reduction of intensity of the 1595 cm^{-1} band and complete attenuation of the band at 1518 cm^{-1}. This is accompanied with the appearance of new NO bands at 1778 and 1848 cm^{-1}. The two weak peaks at 2260 and 2233 cm^{-1} seen for 1.5 and 2.0 L exposure indicate the presence of two distinct N_2O species over this coverage range; however, with increasing exposure only the

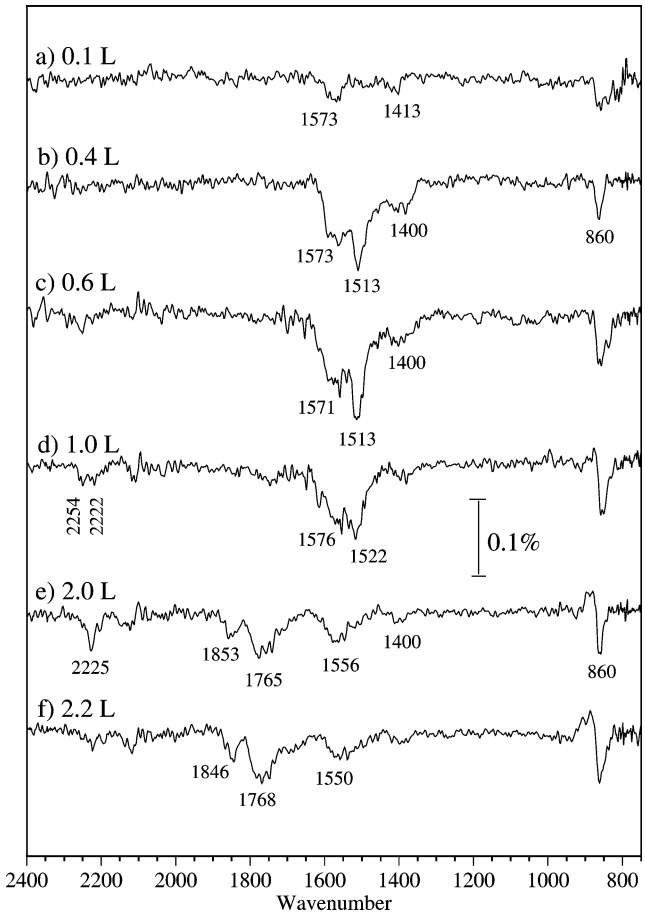

Fig. 3. RAIR spectra following adsorption of NO at 100 K on Cu particles produced from a 0.22 L Cu exposure.

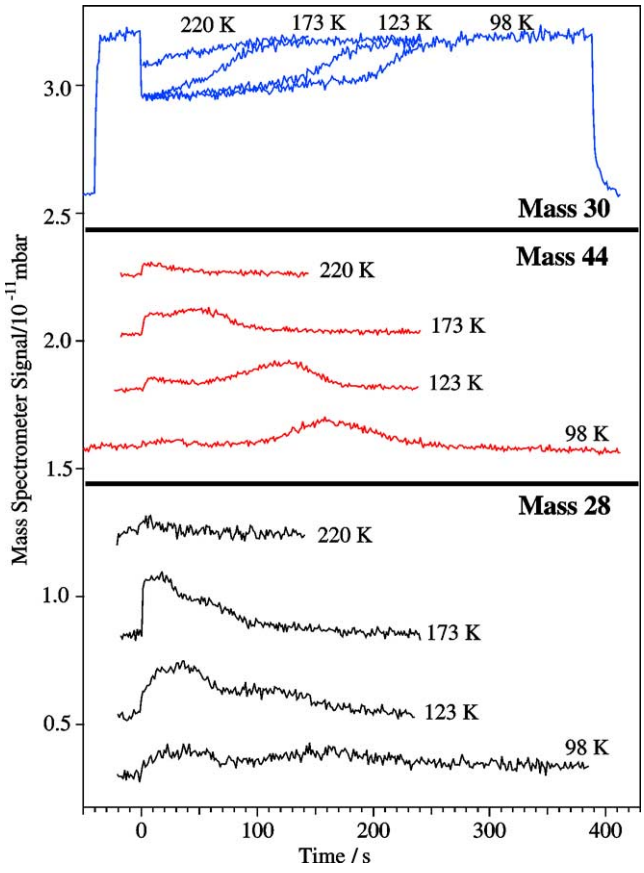

Fig. 4. Isothermal molecular beam scattering experiments showing uptake of NO and evolution of reaction products on a surface preexposed with 1.0 L Cu.

species that gives rise to the lower frequency mode remains on the surface.

The IR spectra from clusters formed with a 0.22 L Cu exposure are shown in Fig. 3. These spectra show a trend similar to those for the higher Cu exposure, with the appearance of multiple NO bands. For the lowest coverage shown two peaks are observed at 1413 and 1573 cm^{-1}, with additional exposure an additional band appears at 1513 cm^{-1}. These bands maximise in intensity at 0.6 L exposure and, subsequently, start to attenuate as new peaks appear at 1765 and 1853 cm^{-1}. As seen before, the 1513 cm^{-1} peak completely vanishes with increasing coverage. The production of N_2O is seen in a manner similar to that observed before, with the appearance of two weak features at 2254 and 2222 cm^{-1} at 1.0 L NO exposure. With an additional 1.0 L exposure the high-frequency component disappears to leave a single peak at 2225 cm^{-1}; however, in this case this also disappears with a small additional exposure.

3.3. Molecular beam experiments

The reactivity of the Cu clusters is illustrated by the molecular beam scattering experiments, which have been measured under conditions identical to those for the IR spectra. Fig. 4 shows the changes in the profiles of masses 28, 30, and 44 for a NO beam scattered from a surface at different temperatures, with clusters formed from a 1.0 L exposure of Cu. The beam initially reflects off an inert flag and strikes the surface at time, $T = 0$. It is clear that the uptake of NO (mass 30) is accompanied by a reaction at the surface resulting in evolution of products into the gas phase with masses 28 and 44 even at temperatures as low as 98 K. The products are identified as $N_2O(44)$ and $N_2(28)$, although it should be noted that the latter is also a cracking fragment of N_2O in the mass spectrometer. The evolution of both gas-phase products seems to appear in two distinct steps, one early and one later in the uptake process. At 98 K, the production of N_2O into the gas phase mainly appears near the completion of the uptake, although with increasing temperature a distinct state appears and increases in size at the start of adsorption. The production of N_2 shows a significant component from the onset of adsorption. Fig. 5 shows the molecular beam scattering results from the clusters formed with a 0.22 L exposure of Cu. The general trend in uptake and production of N_2O and N_2 into the gas phase is similar to that described for the 1.0 L exposure of Cu, the main difference being the reduction of the total uptake and the reduction in N_2 evolution into the gas phase.

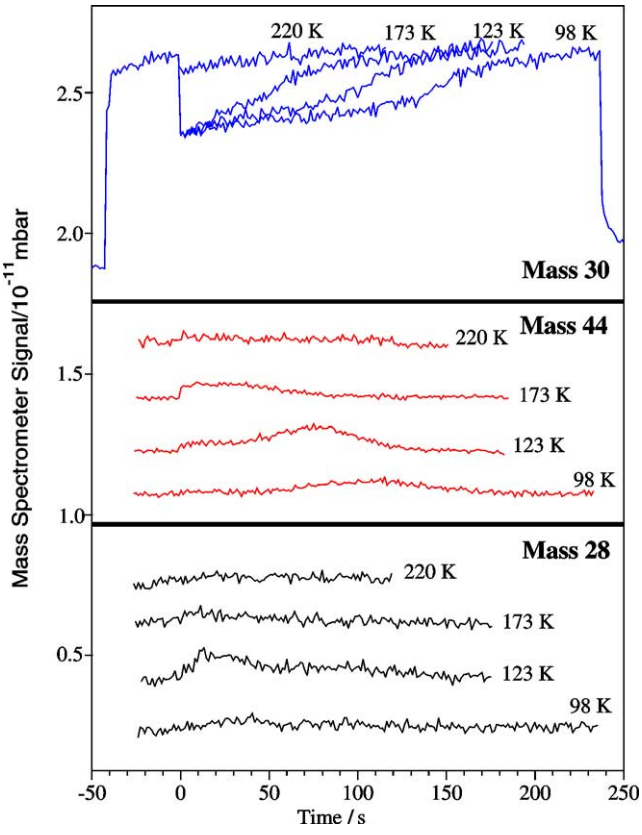

Fig. 5. Isothermal molecular beam scattering experiments showing uptake of NO and evolution of reaction products on a surface preexposed with 0.22 L Cu.

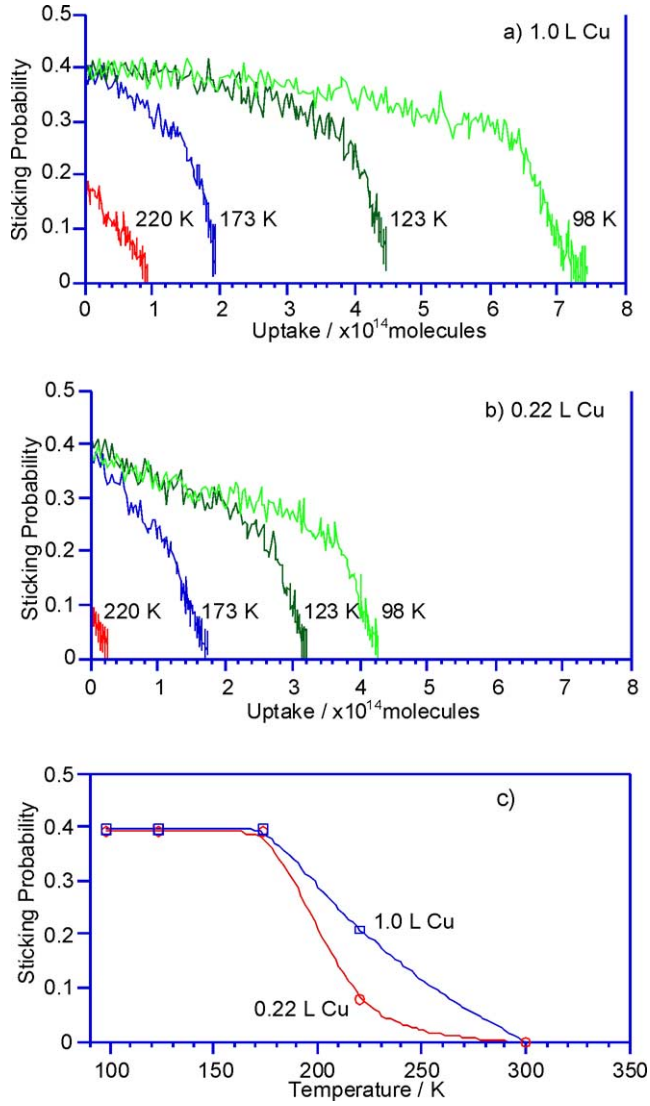

Fig. 6. Variation of the sticking probability with uptake for (a) 1.0 L Cu and (b) 0.22 L Cu. The change of the initial sticking probability with temperature is shown in (c).

The variation in the sticking probability as a function of integrated uptake for the two Cu coverages is shown in Figs. 6a and b. The general trend in these figures shows that between 98 and 173 K the sticking probability falls gradually from an initial value of 0.4 to below 0.25 for a coverage increase of 85% of saturation. Subsequently the sticking rapidly falls to zero. The total uptake steadily decreases with increasing surface temperature. The variation in the initial sticking probability, S_0, with temperature is shown in Fig. 6c. The initial sticking probability stays constant between 93 and 173 K, above this temperature this value decreases to 0.2 at 220 K.

4. Discussion

The adsorption and reactivity of NO on the Cu clusters shows strong similarities to that reported previously for the Cu surfaces, particularly with regard to the formation of N_2 and N_2O at low temperatures. The molecular beam data in particular show near identical behaviour to that observed on the Cu{110} single crystal surface [10]. The Infrared spectra follow the general trend previously reported on both the {110} and the {111} surfaces of Cu, in that the nature of the species resulting from the adsorption of NO changes with increasing coverage. The higher resolution of RAIRS shows three bands in the low coverage regime on the clusters whereas previous HREELS work by Wu and Goodman [8] showed only a single mode at 1520 cm^{-1}.

One particular point of interest that is often generated by vibrational spectra of CO and NO adsorbed on clusters is to determine the adsorption site and to relate this to the appropriate crystalline face of the single crystal counterpart. The adsorption of NO on single crystal surfaces often leads to the observation of multiple bands in the spectral range of 1400–1800 cm^{-1} and in the past each of these has been related to a particular adsorption site, such as atop, twofold bridge, and threefold hollow. There is some evidence that this is sometimes misleading in some NO adsorption systems, as shown in a recent review by Brown and King [3]. In addition, it should be noted that for small clusters, dipole–dipole coupling effects become important and neglecting these can lead to erroneous interpretation, as IR band intensity may not

be directly proportional to concentration of surface species. For large-frequency separation between the bands, as in this case, coupling effects are generally considered to be relatively small. Therefore, with careful analysis and the use of results from previous infrared studies of NO adsorbed on the surfaces of Cu single crystals the vibrational frequencies may be used in the tentative assignment of IR absorption bands to particular site symmetries and hence the morphology of the facets.

Adsorption of NO on Cu{110} shows a single band shifting from 1588 to 1600 cm^{-1} over the low to intermediate coverage range [10]. According to the recent guide by Brown and King [3] this should be assigned to adsorption into threefold sites; however, it was assigned to adsorption in an upright position into twofold bridged sites as the symmetry of the {110} surface precludes upright coordination into threefold sites. The adsorption of NO on Cu{111} over a similar coverage range shows a single band shifting from 1525 to 1560 cm^{-1} and has been assigned to adsorption into threefold sites [9]. The relatively small difference in the upper and lower values of these frequency values makes the translation of these data and hence the site determination on clusters difficult. The IR data from the clusters in this study clearly show the presence of two main bands at about 1586 and 1500 cm^{-1} with a small band at 1409 cm^{-1}. The small size of the latter suggests that this is a minority species and with this assumption is accordingly assigned to adsorption at defect sites such as step or cluster edges. From the aforementioned IR work a tentative assignment of the two main bands is population of twofold bridge and threefold hollow sites for the 1586 and 1500 cm^{-1} bands, respectively. Worren et al. [16] have shown that for clusters > 40 Å the top facet is of (111) orientation. Although, in the first instance the two bands can be assigned to the respective sites on a (111) facet, we note, however, the Cu{111} single crystal surface has both sites available for occupation yet only single (threefold) site occupancy is observed. We, therefore, only attribute the 1500 cm^{-1} band to occupation onto threefold sites on {111} facets. Turning to the 1586 cm^{-1} band it can be seen that our STM data show a range of clusters sizes, which are mostly < 40 Å, the morphology of these have not yet been determined. The IR data imply that these may have adsorption sites that resemble the close packed rows of a {110} surface. If this is the case then adsorption into these sites is energetically favourable as the IR band associated with these appears to be populated and maximise in intensity before population of the {111} terrace sites which give rise to the 1500 cm^{-1} band.

With increasing coverage there is a clear change in the surface species as additional molecules adsorb onto the clusters. The origin of this change needs to be carefully considered. Generally bands observed above 1750 cm^{-1} for adsorbed NO are attributed to adsorption in atop sites, which would simply suggest a change from two- and threefold adsorption sites to atop. However, in light of the previous results the two bands observed at 1768 and 1846 cm^{-1} are similar in frequency and relative intensities as those from a dimerised NO species [10]. Here, the coulombic repulsion associated in coupling two NO molecules is compensated for by the formation of weak N–N bonds with a bond energy of ~ 16 kJ/mol. The structure of the dimer in the gas phase has C_{2v} symmetry. In the gas and condensed phases the $(NO)_2$ dimer is primarily identified by the symmetric (A_1) and asymmetric (B_1) NO-stretching modes at 1860 and 1788 cm^{-1}, respectively, the dynamic dipoles associated with these being perpendicular and parallel to the N–N bond, respectively. The frequency and intensity of these modes may change when the dimer is adsorbed on a surface, as this is mainly governed by the strength of interaction with the surface and its adsorption symmetry or orientation. The modes of adsorption of $(NO)_2$ have been previously discussed in some detail [13].

The orientation of a species adsorbed on a metal surface can be determined from the IR spectra using the dipole selection rule, which dictates that only those vibrations that have a dynamic dipole perpendicular to the surface are IR active. This is also true for supported clusters as the incident light mainly reflects from the underlying NiAl metal substrate and the cluster height indicates that the majority of the cluster surface is coplanar with the substrate. The observation of significant intensity for the υ_a(NO) indicates that the N–N bond is not parallel to the surface plane and thus the dimer bonds in a side-on configuration through one of the NO groups, as observed on Cu{110}. This unusual configuration has previously been reported for $(NO)_2$ adsorbed on graphite [20]. In contrast, on Ag{111} a combination of IR and NEXAFS results showed that the dimer in the monolayer was bonded with its N–N plane parallel to the surface with the N–O plane tilted from the surface normal [13,14]. However, on this surface multilayers of the dimers were all orientated with their N–N bonds perpendicular to the surface plane.

Finally, the two small weak bands observed near 2260 and 2225 cm^{-1} are assigned to υ(N–N) of N_2O. The corresponding (N–O) modes expected between 1280 and 1320 cm^{-1} are of much weaker intensity and hence not observed. The order of appearance of these bands and their frequency are again similar to those previously observed on Cu{110}, both for N_2O adsorbed from the gas phase and for when it was produced from the reaction of NO molecules [10]. The gas-phase value for υ(N–N) is 2224 cm^{-1}. The initial shift in frequency of ~ 36 cm^{-1} has been previously observed on more reactive metals including Pd [21] and Ru [22]. The blue shift indicates a strengthening of the N–N bond through interaction with the surface. The origin of the two bands and the change in intensity remain unclear, although in the case of Cu [10], Pd [21], and Ru [22] the adsorption at 85 K is accompanied by partial dissociation to liberate N_2 into the gas phase and produce coadsorbed atomic oxygen which influences the frequency of the υ(N–N) mode. It is not clear if the appearance of the low-frequency band is associated with a direct interaction with

the adsorbed oxygen or simply associated with a change in adsorption site.

4.1. Adsorption dynamics

The molecular beam data reveal the complex dynamics that are associated with the adsorption of NO on the Cu particles. The data give a detailed insight into the reaction mechanisms which give rise to the changes in the surface species that are observed with RAIRS. It is clear from Fig. 6 that the total integrated uptake changes both as a function of Cu particle coverage and temperature. At 98 K, the total uptake increases by 73% from 0.2 to 1.0 L Cu exposure and reflects the increase in the amount of Cu surface area available for reaction/adsorption.

The changes in the sticking probability as a function of coverage and temperature are typical of precursor-mediated adsorption; that is, incoming molecules trap into an initial precursor state which then leads to either desorption, reaction/dissociation, or chemisorption, depending on the temperature and coverage. The sticking probability is actually a measure of the product of the trapping probability into the precursor state and the probability of transfer from this into the chemisorbed state. The strong decrease in the sticking probability above 200 K indicates that the initial trapping of NO into the precursor state is the one most affected by temperature; i.e., the surface residence time of the NO in the precursor state is temperature dependent. At low temperature it is kinetically transformed to initially adsorbed NO, which subsequently can be transformed to a reaction product. As the temperature of the surface increases, the rate of desorption from the precursor state is greater than the rate of adsorption.

At low temperature the initial sticking probability shows a constant value of 0.4 with both Cu coverages, although the total uptake shows a difference of about 73% between the two. On the Cu{110} single crystal S_0 was measured to be 0.7. The STM results in Fig. 1 show that for the lower Cu coverage used, the clusters decorate mostly domain boundaries and step edges with the terraces mainly free of Cu clusters and it is only with the higher Cu coverage that there is significant population of the terraces. Therefore, in the case of the lower Cu coverage the impinging NO molecules from the beam sample a large surface area which is free of clusters and are interacting with clean alumina, although the reactivity is the same as the higher Cu coverage. However, beam scattering experiments from the clean alumina show no reactive uptake. The implication of this is that the interaction of NO with the clean alumina may not be as weak as the clean surface results would otherwise indicate, as the molecules arriving at the alumina surface are trapped in the precursor state sufficiently long enough for them to diffuse across the surface before finding a reactive Cu site for adsorption. This may be one of the many reasons why supposedly "inert" catalyst supports have an influence on reaction.

4.2. Reactive products

The interaction of the NO beam with the supported clusters is clearly more complex than the simple uptake that may be expected at low temperatures, with the isothermal evolution of N_2 and N_2O into the gas phase during adsorption. It is surprising that the profile of these products is virtually identical to that observed previously on the Cu{110} single crystal [10]. This indicates that the production of these gaseous products from the onset of adsorption at low temperatures is not related to surface crystallography or defects, but inherent of the reaction mechanism. Previous molecular beam and infrared work on N_2O interaction with Cu{110} at 85 K showed that molecular adsorption competes with a dissociative process, which produces gaseous N_2 and adsorbed atomic oxygen [10]. Therefore the production of both N_2O and N_2 gaseous products can be simply related to production of N_2O which in turn has been shown with the IR results to be produced from coupling of two NO molecules to form dimers, as shown by a recent theoretical study [23]. The combination of molecular beam and IR results can therefore be used to establish the reaction mechanisms that are involved in the adsorption process and are outlined below.

$$NO_{(g)} \rightarrow NO^*_{(precursor)}, \tag{1}$$

$$NO^*_{(precursor)} \rightarrow NO_{(ad)}, \tag{2}$$

$$NO_{(ad)} + NO_{(ad)} \rightarrow (N_2O_2)_{(ad)}, \tag{3}$$

$$(N_2O_2)_{(ad)} \rightarrow N_2O_{(ad)} + O_{(ad)}, \tag{4}$$

$$N_2O_{(ad)} \rightarrow N_{2(g)} + O_{(ad)}, \tag{5}$$

$$N_2O_{(ad)} \rightarrow N_2O_{(g)}. \tag{6}$$

To simplify discussion the infrared and molecular beam data are broadly separated into two regimes; low to mid-coverage and mid-coverage to saturation. The mid-coverage is defined in the infrared spectra as the point where the bands between 1500 and 1600 cm^{-1} maximise in intensity, spectrum c in Figs. 2 and 3. In the molecular beam it is defined as the point where the mass 28 signal comes to a minima or plateau after the first maxima.

4.3. Low to mid-coverage range

From the onset of adsorption the infrared shows that three distinct types of NO monomer are produced at 98 K, and that the relative ratios of these change with increasing coverage. The molecular beam behaviour shows that adsorption proceeds via a precursor state, steps (1) and (2) of the reaction mechanism. However, the molecular beam data indicate that some gaseous N_2 and to a lesser extent N_2O are also produced from the start, implying that on chemisorption step (2) is rapidly followed by steps (3)–(5) with some events advancing to step (6). As the surface coverage increases the N_2 signal peaks and subsequently declines. This behaviour is also reflected by the N_2O production but the quantity produced is much lower. The formation of the dimers from the

onset of adsorption suggests that this is not necessarily a result of compression of the overlayer to overcome the steric repulsion generally associated with bringing two molecules close together. Instead, the implication is that there is an attractive interaction between two molecules, which leads to their dimerisation. This is particularly evident at higher temperatures where the increased mobility of the adsorbed molecules would lead to a decrease in the evolution of gaseous products if this were not the case.

The formation of dimers at very low coverages may involve a process which is more complex than that suggested by step (3), as from the combination of IR and molecular beam results it is unlikely that at these coverages the dimers are formed from two chemisorbed NO molecules. Instead a more likely route to dimer formation is that a NO molecule in the highly mobile precursor state interacts directly with a chemisorbed NO molecule. Whether this requires empty next nearest neighbour sites (nn*) adjacent to the already chemisorbed NO cannot be directly deduced from the data. Therefore step (3) of the overall mechanism should be modified for the low coverage regime as consisting of the two following steps:

$$NO^*_{(precursor)} + NO_{(ad)} \rightarrow N_2O_{2(ad)}, \quad (3a)$$

$$NO^*_{(precursor)} + nn^* + NO_{(ad)} \rightarrow N_2O_{2(ad)}. \quad (3b)$$

An indication of which of these two channels is the most probable comes again from closer inspection of both the IR and the molecular beam data at 98 K. Over the low coverage range the dimer or its decomposition product N_2O is never observed on the surface in the IR. This suggests that the dimer is highly reactive on the surface at low coverages and initially produces N_2O and adsorbed atomic O, the latter clearly requires an empty next nearest neighbour site. The molecular beam shows that the majority of the N_2O must be immediately decomposing into N_2 and atomic O, while the remainder desorbs. Thus overall two empty next nearest neighbours are required to accommodate the two O adatoms. With increasing uptake, the fulfilling of this requirement becomes more unlikely, so very quickly after the onset of adsorption it may be expected that this reaction route becomes passivated. This is essentially what is seen in the molecular beam data and suggests that step (3b) is the most probable in describing the low coverage observation.

The evidence from the molecular beam for the production of coadsorbed atomic O suggests the IR spectra should be reinterpreted to account for any influence of this coadsorbate. Although it is well known that in many systems coadsorbed O does influence the adsorption site and frequency of both CO and NO, in this case for the low coverage regime the influence of any interaction on the vibrational frequency may be minimal. The main evidence for this comes from examination of the IR spectra from the NO adsorbed on Cu{111} and {110} surfaces over a similar coverage regime, where a single band is observed, although coadsorbed O is certainly present in the case of the latter and, by inference, presumably in the former.

There is a clear increase in the N_2 and N_2O signals with increasing temperature; the signals show a maxima at 173 K and subsequently decrease. These observations are consistent with the mechanism outlined above. The increase in the signals can be simply related to an increased rate of desorption of the products (steps (5) and (6)) as at these temperatures the surface species are not stable and desorb immediately on formation. More significantly, there is an increase in the amount of N_2O produced at 173 K compared to lower temperatures. This can be related to two different processes: First it may simply be related to the increased production of N_2 which would result in an increase in the accumulation of surface oxygen which limits the further decomposition of N_2O and leads to its desorption. Alternatively, it could be directly ejected into the gas phase from the transition state that dissociates the dimer intermediate; i.e., the surface residence time of this species is so low that it never experiences an interaction with the surface. The change in the relative ratio of N_2 and N_2O on increasing the temperature from 123 to 220 K indicates that it is likely both these processes are occurring simultaneously although the latter becomes more prominent at 220 K.

4.4. Mid-coverage to saturation range

The changes in both the infrared and the molecular beam data over the mid to saturation coverage range are directly related to the compression of the chemisorbed surface species with increased adsorption. The infrared spectra show the reduction of intensity of the bands associated with adsorbed monomers; this is accompanied by the simultaneous appearance of new bands, which have been assigned to adsorbed N_2O and NO dimers. Therefore the adsorbed monomers must be directly converted into these new species. During this process the molecular beam shows the evolution of both N_2O and N_2. At 98 K, the relative ratio of these is different from that observed for the low coverage regime, with a significantly larger fraction of N_2O produced. The maxima of the gaseous N_2O occur toward the end of the uptake. These changes can be directly related to the number of empty sites available to accommodate both molecular and dissociative adsorption. At the mid-coverage range a mixture of atomic oxygen and molecular NO is adsorbed on the surface of the Cu clusters; the adsorption of additional NO from the extrinsic precursor state to form dimers can proceed either through step (3) or (3a), as in both cases the monomeric species are converted to the dimer. The subsequent fate of the dimer is determined by the local surface population; if an empty site is available then the dimer may decompose to produce N_2O and atomic O. However, the probability of the N_2O decomposing further is limited by the availability of finding an additional empty site. This becomes progressively difficult as the surface gets saturated with molecular and atomic species and results in the decomposition of the dimer to produce N_2O which can either desorb into the gas phase or remain adsorbed without further decomposition. Eventually

the dimer becomes stable on the surface presumably due to the lack of empty sites that are available for decomposition.

5. Conclusion

The adsorption and reaction of NO on Cu clusters deposited on a 5 Å thick Al_2O_3 film created by oxidation of NiAl{110} shows strong similarities to its behaviour on Cu single crystals. A combination of infrared and molecular beam data shows a complex reaction mechanism. The STM results show that the Cu clusters grow according to the Volmer–Weber mechanism and initially decorate mainly antiphase domain boundaries and step edges. The mean cluster size ranges from 20 to 40 Å and is typically 6–8 Å in height. The IR spectra at low coverage shows two main bands at 1586 and 1500 cm^{-1} associated with two distinct monomeric NO species, adsorbed in twofold bridge and threefold hollow sites on particles with facets which resemble (110) and (111) surfaces, respectively. At higher coverage these monomeric species are converted into dimeric NO and N_2O species, identified by vibarational bands at 1778 and 2230 cm^{-1}. The N_2O is directly formed from the (NO)2 dimer. Molecular beam measurements show that N_2O is produced from the onset of adsorption; however, it initially dissociates to produce gas phase N_2 and O_{ad}. At higher coverages this dissociation is inhibited and while some N_2O is observed on the surface some desorbs into the gas phase.

Acknowledgments

The EPSRC is acknowledged for equipment grants (GR/L93942), a studentship for A.C., and a postdoctoral fellowship for S.H.

References

[1] M. Bäumer, H.-J. Freund, Prog. Surf. Sci. 61 (1999) 127.
[2] K.C. Taylor, Catal. Rev. Sci. Eng. 35 (1993) 457.
[3] W.A. Brown, D.A. King, J. Phys. Chem. B 104 (2000) 2578.
[4] M.H. Matloob, M.W. Roberts, J. Chem. Soc. Faraday Trans. 73 (1977) 1393.
[5] D.W. Johnson, M.H. Matloob, M.W. Roberts, J. Chem. Soc. Faraday Trans. 75 (1979) 2143.
[6] J.F. Wendelken, J. Vac. Sci. Technol. 20 (1982) 884.
[7] J.F. Wendelken, App. Surf. Sci. 11/12 (1982) 172.
[8] M.C. Wu, D.W. Goodman, J. Phys. Chem. 98 (1994) 9874.
[9] P. Dumas, M. Suhren, Y.J. Chabal, C.J. Hirschmugl, G.P. Williams, Surf. Sci. 371 (1997) 200.
[10] W.A. Brown, R.K. Sharma, D.A. King, S. Haq, J. Phys. Chem. 100 (1996) 12559.
[11] C.M. Kim, C.W. Yi, D.W. Goodman, J. Phys. Chem. B 106 (2002) 7065.
[12] S.K. So, R. Franchy, W. Ho, J. Chem. Phys. 95 (1991) 1385.
[13] W.A. Brown, P. Gardner, D.A. King, J. Phys. Chem. 99 (1995) 7065.
[14] W.A. Brown, P. Gardner, M. Perez-Jigato, D.A. King, J. Chem. Phys. 102 (1995) 7277.
[15] R.M. Jaeger, H. Kuhlenbeck, H.-J. Freund, M. Wuttig, W. Hoffmann, R. Franchy, H. Ibach, Surf. Sci. 259 (1991) 235.
[16] T. Worren, K.H. Hansen, E. Laegsgaard, F. Besenbacher, I. Stensgaard, Surf. Sci. 477 (2001) 8.
[17] C. Winkler, A. Carew, J. Ledieu, R. McGrath, R. Raval, Surf. Rev. Lett. 8 (2001) 693.
[18] C.L. Pang, H. Raza, S.A. Haycock, G. Thornton, Surf. Sci. 460 (2000) L510.
[19] M. Frank, K. Wolter, N. Magg, M. Heemeier, R. Kuhnemuth, M. Baumer, H.-J. Freund, Surf. Sci. 492 (2001) 270.
[20] J. Suzanne, J.P. Coulomb, M. Bienfait, M. Matecki, A. Thomy, B. Croste, C. Marti, Phys. Rev. Lett. 41 (1978) 760.
[21] S. Haq, A. Hodgson, Surf. Sci. 463 (2000) 1.
[22] E. Umbach, D. Menzel, Chem. Phys. Lett. 84 (1981) 491.
[23] Y. Zhanga, Y. Suna, A. Caoa, J. Liua, G. Fan, J. Mol. Struct. (Theochem.) 623 (2003) 245.